GUT-inspired supersymmetric model for h→γγ and the muon g-2

M. Adeel Ajaib, Ilia Gogoladze, and Qaisar Shafi

Phys. Rev. D **91**, 095005 — Published 6 May 2015

DOI: 10.1103/PhysRevD.91.095005

GUT-Inspired Supersymmetric Model for $h \to \gamma\gamma$ and Muon $g-2$

M. Adeel Ajaib[a,1], Ilia Gogoladze[b,2], and Qaisar Shafi[b,3]

[a] *Department of Physics and Astronomy, Ursinus College, Collegeville, PA 19426*

[b] *Bartol Research Institute, Department of Physics and Astronomy, University of Delaware, Newark, DE 19716, USA*

Abstract

We study a GUT-inspired supersymmetric model with non-universal gaugino masses that can explain the observed muon $g-2$ anomaly while simultaneously accommodating an enhancement or suppression in the $h \to \gamma\gamma$ decay channel. In order to accommodate these observations and $m_h \simeq 125-126$ GeV, the model requires a spectrum consisting of relatively light sleptons whereas the colored sparticles are heavy. The predicted stau mass range corresponding to $R_{\gamma\gamma} \geq 1.1$ is 100 GeV $\lesssim m_{\tilde{\tau}} \lesssim$ 200 GeV. The constraint on the slepton masses, particularly on the smuons, arising from considerations of muon $g-2$ is somewhat milder. The slepton masses in this case are predicted to lie in the few hundred GeV range. The colored sparticles turn out to be considerably heavier with $m_{\tilde{g}} \gtrsim 4.5$ TeV and $m_{\tilde{t}_1} \gtrsim 3.5$ TeV, which makes it challenging for these to be observed at the 14 TeV LHC.

[1] E-mail: adeel@udel.edu

[2] E-mail: ilia@bartol.udel.edu

On leave of absence from: Andronikashvili Institute of Physics, 0177 Tbilisi, Georgia.

[3] E-mail: shafi@bartol.udel.edu

1 Introduction

The ATLAS and CMS experiments at the LHC have independently reported the discovery [1, 2] of a Standard Model (SM)–like Higgs boson of mass $m_h \simeq 125 - 126$ GeV using the combined 7 TeV and 8 TeV data. This discovery is compatible with low (TeV) scale supersymmetry [3]. At the same time, after the first LHC run we have the following lower bounds on the gluino and squark masses [4, 5]

$$m_{\tilde{g}} \gtrsim 1.4 \text{ TeV (for } m_{\tilde{g}} \sim m_{\tilde{q}}) \quad \text{and} \quad m_{\tilde{g}} \gtrsim 0.9 \text{ TeV (for } m_{\tilde{g}} \ll m_{\tilde{q}}). \tag{1}$$

In some well motivated SUSY models the gluino is the NLSP in which case $m_{\tilde{g}} \gtrsim 400$ GeV [6]. These bounds combined with the bound of 125 GeV on the lightest CP even Higgs boson mass place stringent constraints on the slepton and gaugino (bino or wino) mass spectrum in several well studied scenarios such as constrained MSSM (cMSSM) [7], NUHM1 [8] and NUHM2 [9]. In particular, as we shall show later, in the above mentioned models, the first two generation sleptons are predicted to be more than 1 TeV in order to accommodate the light CP even Higgs with 125 GeV mass. The stau leptons can still be relatively light due to a relatively large trilinear soft supersymmetry breaking (SSB) A-term.

There are several motivations to study models that allow for the sleptons be as light as $\sim$ 100 GeV. For instance, the SM prediction for the anomalous magnetic moment of the muon, $a_\mu = (g-2)_\mu/2$ (muon $g-2$) [10], shows a discrepancy with the experimental results [11]:

$$\Delta a_\mu \equiv a_\mu(\text{exp}) - a_\mu(\text{SM}) = (28.6 \pm 8.0) \times 10^{-10}. \tag{2}$$

If supersymmetry is to offer a solution to this discrepancy, the smuon and gaugino (bino or wino) SSB masses should be $\mathcal{O}(100)$ GeV or so [12]. Thus, it is hard to simultaneously explain the observed Higgs boson mass and resolve the muon $g-2$ anomaly if we consider CMSSM, NUHM1 or NUHM2, since in all these cases, the slepton masses are larger than 1 TeV.

Recently, there have been several attempts to reconcile this apparent tension between muon $g-2$ and the Higgs boson mass within the MSSM framework by assuming non-universal SSB mass terms for the gauginos [13, 14] or the sfermions [15, 16] at the GUT scale. Indeed, a simultaneous explanation of m_h and muon $g-2$ is possible [17] in the presence of $t-b-\tau$ Yukawa coupling unification condition [18]. It has been shown [19] that constraints from FCNC processes are very mild and easily satisfied for the case in which the third generation sfermion masses are split from those of the first two generations. However, if the muon $g-2$ anomaly and the Higgs boson mass are simultaneously explained with non-universal gaugino and/or sfermion masses, the correct relic abundance of neutralino dark matter is typically not obtained [16]. Consistency with the observed dark matter abundance would further constrain the SUSY parameter space.

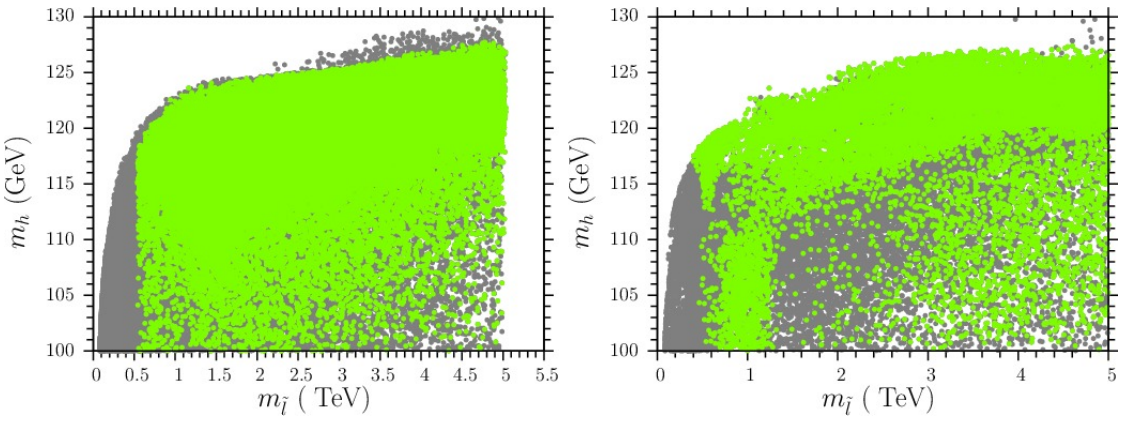

Figure 1: Plots in the m_h vs. $m_{\tilde{l}}$ plane for CMSSM (left panel) and NUHM2 (right panel). *Gray* points are consistent with REWSB and neutralino LSP. *Green* points form a subset of the *gray* points and satisfy the sparticle and Higgs mass bounds, as well as all other constraints described in Section 2.

The Higgs decay channel $h \to \gamma\gamma$ in recent times attracted a fair amount of attention [20] because of the apparent deviation compared to the SM prediction. Currently, the deviation from the SM prediction has significantly reduced but has not completely disappeared. For example, the ATLAS collaboration reported $\mu_{\gamma\gamma} = 1.17 \pm 0.27$ [21], where $\mu_{\gamma\gamma} = \frac{\sigma(pp\to h\to\gamma\gamma)}{\sigma(pp\to h\to\gamma\gamma)^{SM}}$. The CMS collaboration reported a best-fit signal strength in their main analysis $\mu_{\gamma\gamma} = 1.14^{+0.26}_{-0.23}$ [22]. On the other hand, a cut-based analysis by CMS produced $\mu_{\gamma\gamma} = 1.29^{+0.29}_{-0.26}$, which is a slightly different value. This enhancement or suppression in the $h \to \gamma\gamma$ channel with respect to the SM may provide a clue for physics beyond the SM if it is confirmed in the second LHC run. It is known that in order to accommodate an enhancement or suppression in the $h \to \gamma\gamma$ decay channel in the framework of MSSM, the stau is the one of the best candidates, and its mass has to be around 200 GeV or so. It is problematic to accommodate an enhancement or suppression in the $h \to \gamma\gamma$ decay channel in the framework of CMSSM, NUHM1 or NUHM2 models. In this paper we present a GUT inspired model which explains the observed $g-2$ anomaly while simultaneously accommodating an enhancement or suppression in the $h \to \gamma\gamma$ channel.

The paper is organized as follows: In Section 2 we describe the phenomenological constraints and the scanning procedure we implement in our analysis. In Section 3 we provide motivations for the model used in this paper by briefly reviewing the status of the muon $g-2$ anomaly and $h \to \gamma\gamma$ in CMSSM and NUHM2. Our results for the $h \to \gamma\gamma$ channel in the proposed model are presented in Section 4 and for the muon $g-2$ anomaly in Section 5. Our conclusions are outlined in Section 6.

2 Phenomenological Constraints and Scanning Procedure

We employ Isajet 7.84 [23] interfaced with Micromegas 2.4 [24] and FeynHiggs 2.10.0 [25] to perform random scans over the parameter space. In Isajet, the weak scale values of gauge and third generation Yukawa couplings are evolved to $M_{\rm GUT}$ via the MSSM renormalization group equations (RGEs) in the $\overline{DR}$ regularization scheme. We do not strictly enforce the unification condition $g_3 = g_1 = g_2$ at $M_{\rm GUT}$, since a few percent deviation from unification can be assigned to unknown GUT-scale threshold corrections [26]. With the boundary conditions given at $M_{\rm GUT}$, the SSB parameters, along with the gauge and third family Yukawa couplings, are evolved back to the weak scale $M_{\rm Z}$.

In evaluating the Yukawa couplings the SUSY threshold corrections [27] are taken into account at a common scale $M_S = \sqrt{m_{\tilde{t}_L} m_{\tilde{t}_R}}$. The entire parameter set is iteratively run between $M_{\rm Z}$ and $M_{\rm GUT}$ using the full 2-loop RGEs until a stable solution is obtained. To better account for the leading-log corrections, one-loop step-beta functions are adopted for the gauge and Yukawa couplings, and the SSB scalar mass parameters m_i are extracted from RGEs at appropriate scales $m_i = m_i(m_i)$.The RGE-improved 1-loop effective potential is minimized at an optimized scale M_S, which effectively accounts for the leading 2-loop corrections. Full 1-loop radiative corrections are incorporated for all sparticle masses.

We implement the following random scanning procedure: A uniform and logarithmic distribution of random points is first generated in the given parameter space. The function RNORMX [28] is then employed to generate a Gaussian distribution around each point in the parameter space. The data points collected all satisfy the requirement of radiative electroweak symmetry breaking (REWSB), with the neutralino in each case being the LSP.

We use Micromegas to calculate the relic density and $BR(b \to s\gamma)$. The diphoton ratio $R_{\gamma\gamma}$ is calculated using FeynHiggs. After collecting the data, we impose the mass bounds on all the particles [29] and use the IsaTools package [30] to implement the various phenomenological constraints. We successively apply the following experimental constraints on the data that we acquire from ISAJET 7.84:

$$\begin{array}{rll} 123 \text{ GeV} \leq m_h \leq 127 \text{ GeV} & & [1, 2] \\ 0.8 \times 10^{-9} \leq BR(B_s \to \mu^+\mu^-) & \leq 6.2 \times 10^{-9}\ (2\sigma) & [31] \\ 2.99 \times 10^{-4} \leq BR(b \to s\gamma) & \leq 3.87 \times 10^{-4}\ (2\sigma) & [32] \\ 0.15 \leq \frac{BR(B_u \to \tau\nu_\tau)_{\rm MSSM}}{BR(B_u \to \tau\nu_\tau)_{\rm SM}} & \leq 2.41\ (3\sigma). & [32] \end{array}$$

3 Slepton Masses in CMSSM and NUHM2

Before discussing the scenarios where we address the muon $g-2$ anomaly and the decay rate $h \to \gamma\gamma$, we first present the relationship between the light CP even Higgs boson and slepton masses in two well studied models, namely CMSSM and NUHM2. While it is true that radiative corrections to the light CP even Higgs boson mass from the first two family sleptons are negligible, in the following section we show that relations among SSB mass terms from GUT scale boundary conditions in CMSSM and NUHM2 models yield a strong correlation between them. We do not consider the NUHM1 model since it is an intermediate step between CMSSM and NUHM2 in terms of the independent SSB parameters. Therefore, the light CP even Higgs boson mass dependence on slepton masses in NUHM1 can be inferred, more or less, from the CMSSM and NUHM2 models.

We have performed random scans in the fundamental parameter space of CMSSM and NUHM2 with ranges of the parameters given as follows:

$$\begin{aligned} & 0 \leq m_{16} \leq 5\,\text{TeV} \\ & 0 \leq M_{1/2} \leq 3\,\text{TeV} \\ & -3 \leq A_0/m_3 \leq 3 \\ & 35 \leq \tan\beta \leq 55; \\ \text{For CMSSM}: \quad & m_{16} = M_{H_u} = M_{H_d} \\ \text{For NUMH2}: \quad & 0 \leq M_{H_u} \neq M_{H_d} \leq 5\,\text{TeV} \end{aligned} \tag{3}$$

Here m_{16} is the universal SSB mass parameter for sfermions, and $M_{1/2}$ denotes the universal SSB gaugino masses. A_0 is the SSB trilinear scalar interaction coupling, $\tan\beta$ is the ratio of the MSSM Higgs vacuum expectation values (VEVs), and M_{H_u}, M_{H_d} stand for the SSB mass terms for the MSSM up and down Higgs doublets. Since the masses of the light CP even Higgs boson and sleptons do not change significantly for $\tan\beta < 35$, we used data from our former analysis for $35 \leq \tan\beta \leq 55$ to generate Figure 1.

In Figure 1 we display our results in the $m_h - m_{\tilde{l}}$ plane for CMSSM (left panel) and NUHM2 (right panel). Here $m_{\tilde{l}}$ stands for the left handed slepton masses for the first two families. We observe that in the CMSSM and NUHM2 models there is a fairly strong correlation between the Higgs boson mass (m_h) and the first two generation slepton masses ($m_{\tilde{l}}$). Note that the bounds for the right handed slepton masses are very similar and are therefore not displayed. The *gray* points are consistent with REWSB and neutralino LSP, and the *green* points form a subset of the *gray* points and satisfy the sparticle and Higgs mass bounds, as well as all other constraints described in Section 2.

We see from Figure 1 that for both the CMSSM and NUHM2 models, compatibility with the measurement $123\,\text{GeV} \leq m_h \leq 127\,\text{GeV}$ requires that the slepton masses

lie above 1 TeV. The salient features of the results in Figure 1 can be understood by noting that in order for the stop quark mass to be more than 1 TeV [33] (which is necessary to achieve $m_h \approx 125$ GeV), with universal SSB parameters $M_{1/2}$ and m_0, the first and second generation squark masses acquire masses in the multi-TeV range, and the corresponding smuon masses lie around the TeV scale. On the other hand, as mentioned above, in order to have an enhancement in muon $g-2$ and in the decay rate of $h \to \gamma\gamma$, the sleptons need to be much lighter than 1 TeV. Overall, we learn from Figure 1 that in the CMSSM, NUHM1 and NUHM2 scenarios, it is not possible to have enhancement in muon $g-2$ and the decay rate of $h \to \gamma\gamma$ relative to the Standard Model. This conclusion motivates us to explore alternative scenarios which can simultaneously accommodate an enhancement or suppresion of $h \to \gamma\gamma$ and an enhancement in muon $g-2$.

4 $h \to \gamma\gamma$ Decay and Particle Spectra

One of the most promising Higgs boson decay channels is the $\gamma\gamma$ final state which, at leading order, proceeds through a loop containing charged particles, including the charged Higgs, sfermions and charginos. In the SM, the leading contribution to $h \to \gamma\gamma$ decay comes from the W boson loop, the top loop being the next dominant one. The decay width is given by (see [34, 35] and references therein)

$$\Gamma(h \to \gamma\gamma) = \frac{G_F \alpha^2 m_h^3}{128\sqrt{2}\pi} \left| N_c\, Q_t^2\, g_{htt}\, A_{1/2}^h(\tau_t) + g_{hWW}\, A_1^h(\tau_W) + \mathcal{A}_{\rm SUSY}^{\gamma\gamma} \right|^2, \quad (4)$$

where g_{hWW} is the coupling of h to the W boson. The supersymmetric contribution $\mathcal{A}_{\rm SUSY}^{\gamma\gamma}$ is given by

$$\mathcal{A}_{\rm SUSY}^{\gamma\gamma} = g_{hH^+H^-} \frac{m_W^2}{m_{H^\pm}^2} A_0^h(\tau_{H^\pm}) + \sum_f N_c Q_f^2\, g_{h\tilde{f}\tilde{f}} \frac{m_Z^2}{m_{\tilde{f}}^2} A_0^h(\tau_{\tilde{f}}) + \sum_i g_{h\chi_i^+\chi_i^-} \frac{m_W}{m_{\chi_i}} A_{\frac{1}{2}}^h(\tau_{\chi_i}), \quad (5)$$

where g_{hXX} is the coupling of h to the particle X $(= H^\pm, \tilde{f}, \chi_i^\pm)$.

The stop and sbottom loop factors have similar contributions as the gluon fusion case. In this case, however, the stau can also contribute to enhance the decay width without changing the gluon fusion cross section. The chargino contribution to the decay width is known to be less than 10% for $m_{\chi_i^\pm} \gtrsim 100$ GeV. The charged Higgs contribution is even smaller since its coupling to the CP-even Higgs is not proportional to its mass and also due to the loop suppression $m_W^2/m_{H^\pm}^2$.

In the MSSM framework it was shown [20] that only a light stau can give significant enhancement/suppresion in the process $gg \to h \to \gamma\gamma$, while keeping the lightest CP-even Higgs boson mass in the interval 123 GeV $\leq m_h \leq$ 127 GeV.

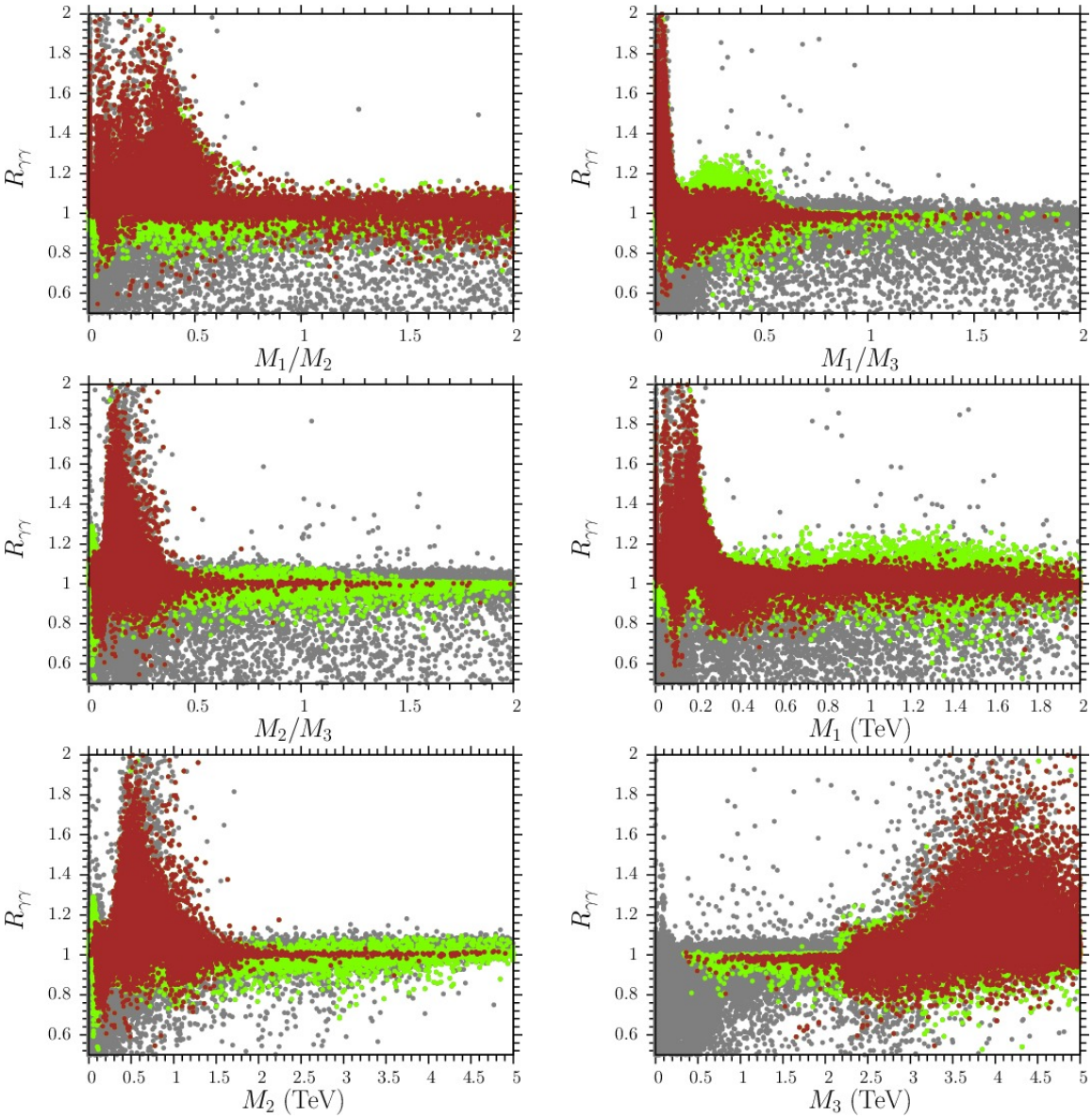

Figure 2: Plots in the $R_{\gamma\gamma} - M_1/M_2$, $R_{\gamma\gamma} - M_1/M_3$, $R_{\gamma\gamma} - M_2/M_3$, $R_{\gamma\gamma} - M_1$, $R_{\gamma\gamma} - M_2$ and $R_{\gamma\gamma} - M_3$ planes. *Gray* points are consistent with REWSB and neutralino LSP. *Green* points form a subset of the *gray* points and satisfy the sparticle and Higgs mass bounds, as well as all other constraints described in Section 2. *Brown* points belong to a subset of *green* points and satisfy the following bound on the LSP neutralino relic abundance, $0.001 \leq \Omega h^2 \leq 1$.

In this paper we discuss the scenario with non-universal and opposite sign gaugino masses at $M_{\rm GUT}$, while the sfermion masses at M_{GUT} assumed to be universal. This is a follow up of the work presented in ref. [13], where it was shown that the muon $g-2$ anomaly can be explained in this model, but the decay rate for $h \to \gamma\gamma$ was not analyzed. It was shown in ref. [13] that the sleptons can be as light as 100 GeV in this model. This observation motivated us to investigate the decay rate for $h \to \gamma\gamma$ and study the parameter space which yields enhancement or suppression for this process.

We perform random scans for following ranges of the parameters:

$$\begin{aligned} 0 \leq m_{16} &\leq 3\,\text{TeV} \\ 0 \leq M_1 &\leq 5\,\text{TeV} \\ 0 \leq M_2 &\leq 5\,\text{TeV} \\ -5 \leq M_3 &\leq 0\,\text{TeV} \\ -3 \leq A_0/m_{16} &\leq 3 \\ 2 \leq \tan\beta &\leq 60 \\ 0 \leq m_{10} &\leq 5\,\text{TeV} \\ \mu &> 0. \end{aligned} \tag{6}$$

Here M_1, M_2, and M_3 denote the SSB gaugino masses for $U(1)_Y$, $SU(2)_L$ and $SU(3)_c$ respectively. We choose different sign for gauginos which was again motivated from the work presented in ref [13], where it was shown that an opposite sign non-universal gaugino mass case is more preferable from the muon $g-2$ point of view than the same sign non-universal gaugino case.

The main message of Section 3 is that with universal SSB mass terms for the gaugino and sfermion sectors, it is impossible to have significant SUSY contributions to the decay $h \to \gamma\gamma$ and muon $g-2$. On the other hand, as shown in ref. [13], non-universal gaugino masses allow for sufficiently light sleptons while keeping the colored sparticles in the multi TeV region. Because of this observation, we investigate the extent to which non-universality is allowed in the gaugino sector to enhance or suppress the decay channel $h \to \gamma\gamma$. The color coding in Figure 2 is given as follows, *Gray* points are consistent with REWSB and neutralino LSP. *Green* points form a subset of the *gray* points and satisfy the sparticle and Higgs mass bounds, as well as all other constraints described in Section 2. *Brown* points belong to a subset of *green* points and satisfy the constraint $0.001 \leq \Omega h^2 \leq 1$ on the LSP neutralino relic abundance. We have chosen to display our results for a wider range of Ωh^2, keeping in mind that one can always find points compatible with the current WMAP range for relic abundance with dedicated scans within the brown regions.

The results from the $R_{\gamma\gamma} - M_1/M_2$, $R_{\gamma\gamma} - M_1/M_3$ and $R_{\gamma\gamma} - M_2/M_3$ planes show that a significant deviation from universality of gaugino masses in order to have sizable SUSY contribution to $h \to \gamma\gamma$ decay is necessary. For instance, the ratio

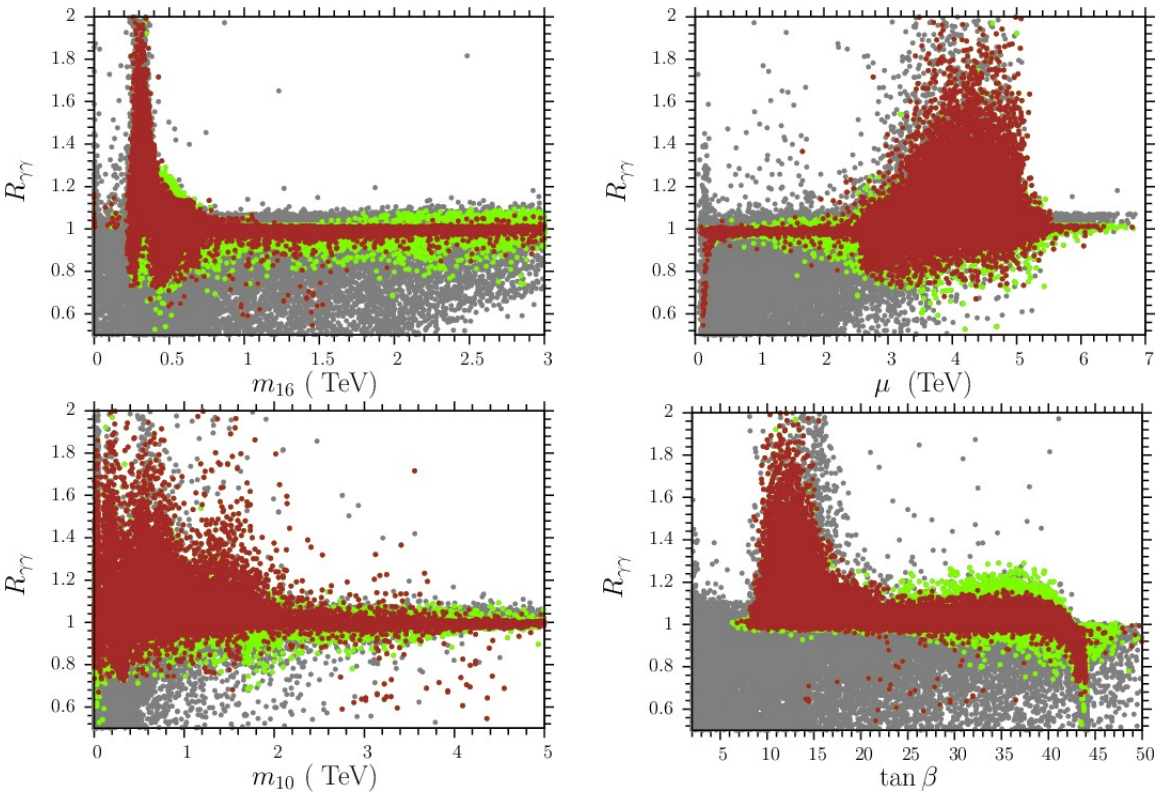

Figure 3: Plots in the $R_{\gamma\gamma} - m_{16}$, $R_{\gamma\gamma} - \mu$, $R_{\gamma\gamma} - m_{10}$ and $R_{\gamma\gamma} - \tan\beta$ planes. Color coding same as in Figure 2.

M_1/M_3 needs to be more than 5, while $M_2/M_3 > 3$ and $M_1/M_2 > 2$. Not only do we observe a strict prediction of gaugino mass ratios, but also a precise prediction of their values. In particular, from the $R_{\gamma\gamma} - M_1$ panel we can see that it is difficult to have an enhancement of $h \to \gamma\gamma$ if $M_1 \gtrsim 300$ GeV. At the same time, the upper bound on M_2 is less stringent and enhancement of $h \to \gamma\gamma$ occurs even with M_2 around 1 TeV.

We observe from the $R_{\gamma\gamma} - M_3$ panel that the parameter $M_3 \gtrsim 2.5$ TeV. The reason for such a large value of M_3 is the following. Since we assume universality in sfermion masses and seek solutions with sleptons not heavier than a few hundred GeV, m_{16} is required to be around a few hundred GeV. Moreover, with a tau slepton mass of around a hundred GeV, in order to avoid breaking the charge symmetry, A_τ needs to be around a hundred GeV. This places a constraint on A_t because we assume a universal trilinear SSB A_0 term. Consequently, a relatively small value of A_t is obtained at low scale. On the other hand, it was shown in [33] that the stop mass needs to be more than 3 TeV if A_t is not the dominant contributor to the radiative corrections of the light CP-even Higgs boson mass. In order to obtain such a heavy stop quark, when m_{16} is of order hundred GeV, a fairly large M_3 is required. This tendency can be observed from the following semi-analytic expressions for stop quark masses [36]

$$\begin{aligned} m^2_{Q_t} &\approx 5.41M_3^2 + 0.392M_2^2 + 0.64m_{16}^2 + 0.115M_3A_{t_0} - 0.072M_3M_2 + \ldots, \\ m^2_{U_t} &\approx 4.52M_3^2 - 0.188M_2^2 + 0.273m_{16}^2 - 0.066A_{t_0}^2 - 0.145M_3M_2 + \ldots. \end{aligned} \tag{7}$$

It is clear from Eq. (7) that if m_{16}, M_2 and A_t are of the order of hundred GeV or so, the way to obtain several TeV stop quark masses is to also have M_3 around several TeV.

In Figure 3 we display our results for the fundamental parameters in the $R_{\gamma\gamma} - m_{16}$, $R_{\gamma\gamma} - \mu$, $R_{\gamma\gamma} - m_{10}$ and $R_{\gamma\gamma} - \tan\beta$ planes. We can see that an enhancement in the $h \to \gamma\gamma$ channel constrains the parameters in this model. The fundamental parameter m_{16} is restricted to a narrow range, 200 GeV $\lesssim m_{16} \lesssim$ 600 GeV, for $R_{\gamma\gamma} \geq 1.1$. Similarly, the range for the other parameters for a corresponding enhancement in the $h \to \gamma\gamma$ channel are: 2.5 TeV $\lesssim \mu \lesssim$ 5.5 TeV, $m_{10} \lesssim 2$ TeV, $10 \lesssim \tan\beta \lesssim 20$.

Figure 4 shows our results for the sparticle masses in the $R_{\gamma\gamma} - m_{\tilde{\tau}}$, $R_{\gamma\gamma} - m_{\tilde{\chi}_1^0}$, $R_{\gamma\gamma} - m_{\tilde{g}}$ and $R_{\gamma\gamma} - m_{\tilde{t}_1}$ planes. For $R_{\gamma\gamma} \geq 1.1$, the stau and the neutralino are both relatively light with mass ranges 100 GeV $\lesssim m_{\tilde{\tau}} \lesssim$ 200 GeV and 50 GeV $\lesssim m_{\tilde{\chi}_1^0} \lesssim$ 200 GeV. From the lower panels of Figure 4 we can see that the colored sparticles corresponding to $R_{\gamma\gamma} \geq 1.1$ are heavy with $m_{\tilde{g}} \gtrsim 4.5$ TeV and $m_{\tilde{t}_1} \gtrsim 3.5$ TeV. The reason for such heavy stop and gluino masses has been discussed above. Testing squarks and gluinos with this mass would be challenging at 14 TeV LHC.

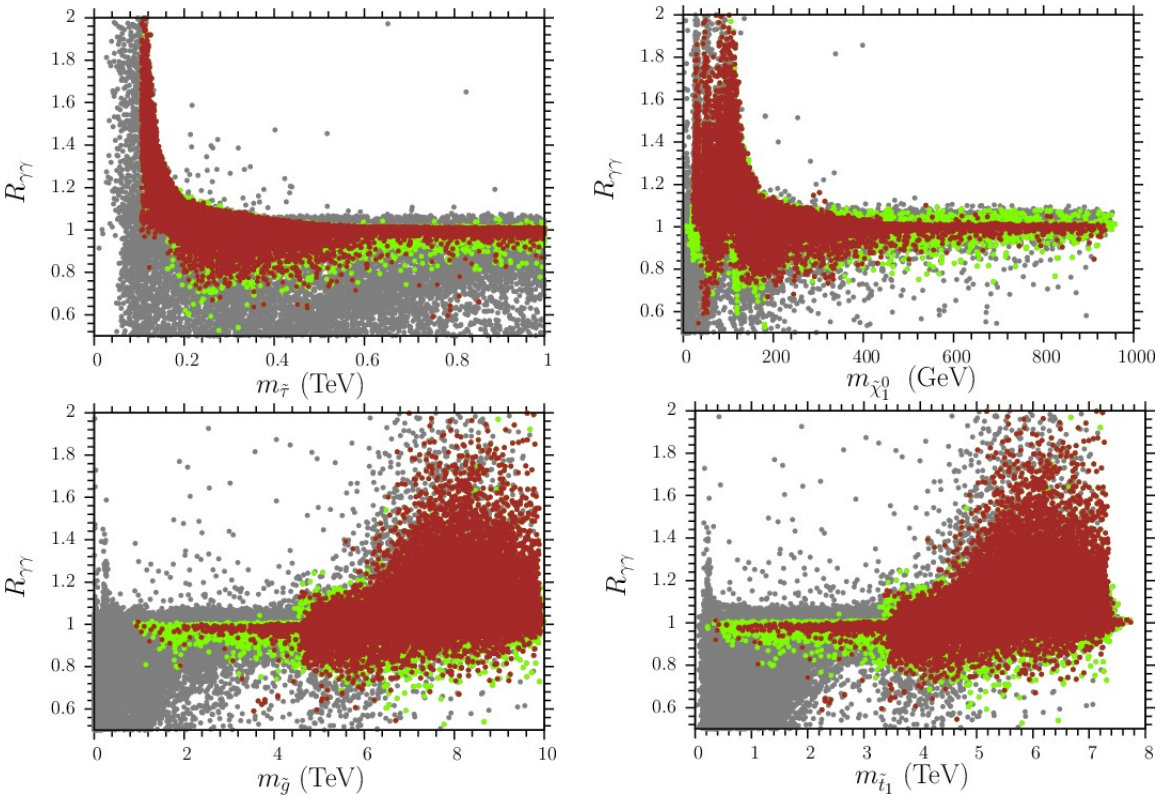

Figure 4: Plots in the $R_{\gamma\gamma} - m_{\tilde{\tau}}$, $R_{\gamma\gamma} - m_{\tilde{\chi}_1^0}$, $R_{\gamma\gamma} - m_{\tilde{g}}$ and $R_{\gamma\gamma} - m_{\tilde{t}_1}$ planes. Color coding same as in Figure 2.

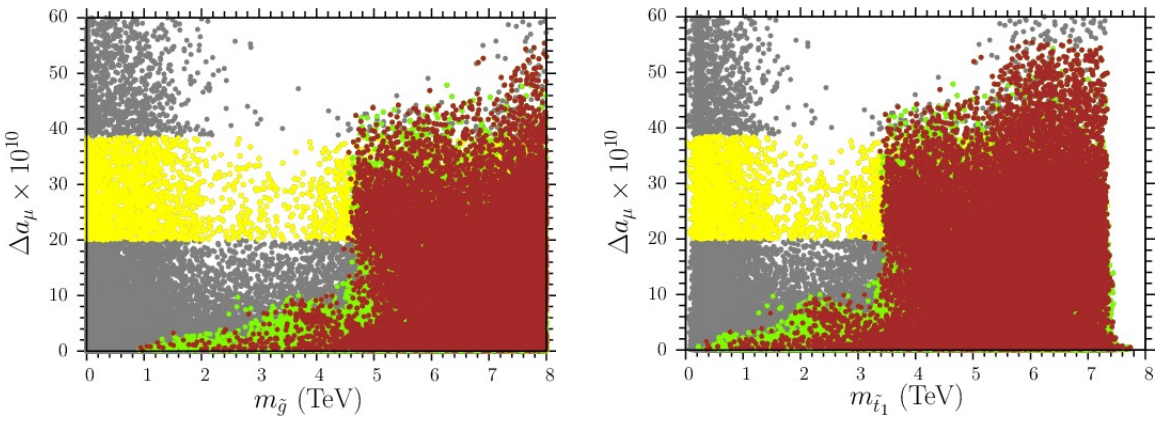

Figure 5: Plots in the $\Delta a_\mu - m_{\tilde{g}}$ and $\Delta a_\mu \times 10^{10} - m_{\tilde{t}_1}$ planes. Color coding same as in Figure 2.

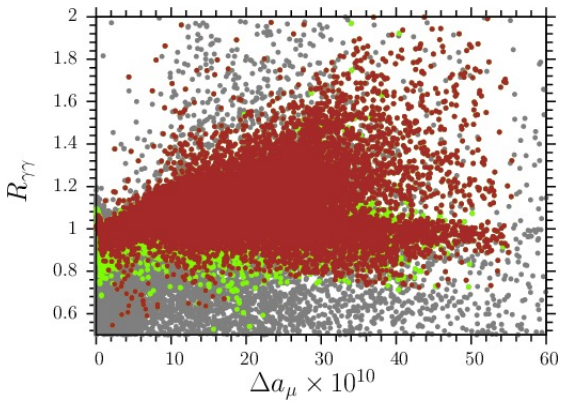

Figure 6: Plot in the the $R_{\gamma\gamma} - \Delta a_\mu$ plane. Color coding same as in Figure 2.

5 The Muon Anomalous Magnetic Moment

The leading contribution from low scale supersymmetry to the muon anomalous magnetic moment [12] depends on the following parameters:

$$M_1,\ M_2,\ \mu,\ \tan\beta, m_{\tilde{\mu}_L},\ m_{\tilde{\mu}_R}, \tag{8}$$

Since we assume a universal the trilinear SSB term A_0, it follows that $A_\mu < \mu \tan\beta$ and we therefore do not consider the trilinear SSB-term contribution here.

The colored particles do not directly provide significant contribution to the muon $g-2$ calculation but are still constrained from the bound on the light CP even Higgs boson mass and the muon $g-2$ calculation. Figure 5 shows our results in the $\Delta a_\mu \times 10^{10} - m_{\tilde{g}}$ and $\Delta a_\mu \times 10^{10} - m_{\tilde{t}_1}$ planes. We can see that the above mentioned constraint yields a stringent lower bound for the gluino and stop masses. Both these sparticles have to be heavier than 3 TeV, which makes it very hard to see them in the second LHC run. However, there is hope that these sparticles can be observed at a future 100 TeV collider.

In Figure 6 we display results in the $R_{\gamma\gamma} - \Delta a_\mu$ plane. The plot shows that there is a considerable region of the parameter space that allows for simultaneous enhancement in the decay channel $h \to \gamma\gamma$ and muon $g-2$. In this model we can have the correct neutralino dark matter relic abundance through the slepton coannihilation channel. It is also interesting that this model connects the parameter space relevant for two different experiments. If the enhancement in the $h \to \gamma\gamma$ decay channel is excluded than a considerable region of the parameter space that explains the $g-2$ anomaly will also be excluded.

Finally, in Table 1 we display four benchmark points from our analysis. All these points satisfy the constraints described in section 2. The first and third point yield a muon $g-2$ around the central measured value with $R_{\gamma\gamma} = 1.2$ and $R_{\gamma\gamma} = 1.0$,

	Point 1	Point 2	Point 3	Point 4
m_{16}	351	438	561	392
m_{10}	451	32	478	2.7
A_0/m_{16}	-2.6	1.6	0.3	2.6
$\tan\beta$	12	26	42	43
M_1	88	5	344	749
M_2	714	1051	124	722
M_3	-4913	-4550	-4420	-4524
μ	471	747	680	811
m_h	123	124	124	125
m_H	4847	4074	1607	591
m_A	4815	4047	1596	587
$m_{H^\pm}$	4847	4075	1610	600
$m_{\tilde{\chi}^0_{1,2}}$	$75, 720$	$33, 999$	$184, 198$	$367, 712$
$m_{\tilde{\chi}^0_{3,4}}$	$4774, 4774$	$4570, 4570$	$4512, 4513$	$4628, 4628$
$m_{\tilde{\chi}^\pm_{1,2}}$	$726, 4729$	$1004, 4528$	$199, 4470$	$714, 4585$
$m_{\tilde{g}}$	9709	9029	8857	9008
$m_{\tilde{u}_{L,R}}$	$8247, 8262$	$7703, 7697$	$7553, 7582$	$7674, 7689$
$m_{\tilde{t}_{1,2}}$	$7217, 7800$	$6664, 7146$	$6573, 6707$	$6625, 6754$
$m_{\tilde{d}_{L,R}}$	$8247, 8269$	$7704, 7703$	$7553, 7588$	$7675, 7692$
$m_{\tilde{b}_{1,2}}$	$7756, 8208$	$7107, 7432$	$6613, 6750$	$6608, 6750$
$m_{\tilde{\nu}_1}$	410	727	446	543
$m_{\tilde{\nu}_3}$	419	728	677	813
$m_{\tilde{e}_{L,R}}$	$561, 150$	$787, 354$	$469, 549$	$552, 449$
$m_{\tilde{\tau}_{1,2}}$	$176, 519$	$160, 786$	$368, 892$	$526, 979$
$\Delta(g-2)_\mu$	29.5×10^{-10}	4.67×10^{-10}	29.3×10^{-10}	29.4×10^{-10}
$R_{\gamma\gamma}$	1.2	1.1	1	0.74

Table 1: Four benchmark points from our analysis. The first point has $R_{\gamma\gamma} = 1.2$ with the central value of $g-2$. The second point has $(g-2)_\mu$ consistent with the SM and $R_{\gamma\gamma} = 1.1$. The third point also has the central value of $(g-2)_\mu$ but with no enhancement in the diphoton channel. The fourth point shows a suppression in the diphoton channel with $R_{\gamma\gamma} = 0.74$. For all these points the sleptons are relatively light but the colored sparticles are considerably heavier.

respectively. The second point has $(g-2)_\mu$ consistent with the SM and $R_{\gamma\gamma} = 1.1$. The fourth point shows a suppression in the diphoton channel with $R_{\gamma\gamma} = 0.74$. For all these points the sleptons are light while the colored sparticles are considerably heavier.

6 Conclusion

We studied a supersymmetric model with non-universal gaugino masses at M_{GUT} that accommodates enhancement or suppression in the $h \to \gamma\gamma$ channel while simultaneously explaining the muon $g-2$ anomaly. The parameter space we obtain is consistent with the current bounds on the sparticle masses and constraints from B-physics. The desired neutralino dark matter relic abundance is achieved in this model through slepton coannihilation channel. We find that the parameter space with $R_{\gamma\gamma} \geq 1.1$ predicts relatively light sleptons with a stau mass range of 100 GeV $\lesssim m_{\tilde{\tau}} \lesssim$ 200 GeV. The colored sparticles corresponding to $R_{\gamma\gamma} \geq 1.1$ are heavy with $m_{\tilde{g}} \gtrsim 4.5$ TeV and $m_{\tilde{t}_1} \gtrsim 3.5$ TeV, which makes it very challenging to observe them in the second run of LHC.

Acknowledgments

This work is supported in part by the DOE Grant No. DE-FG02-12ER41808. This work used the Extreme Science and Engineering Discovery Environment (XSEDE), which is supported by the National Science Foundation grant number OCI-1053575. I.G. acknowledges support from the Rustaveli National Science Foundation No. 03/79.

References

[1] G. Aad *et al.* [ATLAS Collaboration], Phys. Lett. B **716**, 1 (2012).

[2] S. Chatrchyan *et al.* [CMS Collaboration], Phys. Lett. B **716**, 30 (2012).

[3] See, for instance, S. P. Martin, arXiv:hep-ph/9709356 [hep-ph] and references therein.

[4] G. Aad *et al.* [ATLAS Collaboration], Phys. Rev. D **87**, 012008 (2013).

[5] S. Chatrchyan *et al.* [CMS Collaboration], JHEP **1210**, 018 (2012).

[6] I. Gogoladze, R. Khalid and Q. Shafi, Phys. Rev. D **80**, 095016 (2009); M. A. Ajaib, T. Li and Q. Shafi, Phys. Lett. B **705**, 87 (2011); S. Raza, Q. Shafi and C. S. n, arXiv:1412.7672 [hep-ph].

[7] G. L. Kane, C. F. Kolda, L. Roszkowski and J. D. Wells, Phys. Rev. D **49**, 6173 (1994).

[8] H. Baer, A. Mustafayev, S. Profumo, A. Belyaev and X. Tata, Phys. Rev. D **71**, 095008 (2005).

[9] J. Ellis, K. Olive and Y. Santoso, *Phys. Lett.* **B 539** (2002) 107; J. Ellis, T. Falk, K. Olive and Y. Santoso, *Nucl. Phys.* **B 652** (2003) 259; H. Baer, A. Mustafayev, S. Profumo, A. Belyaev and X. Tata, *J. High Energy Phys.* **0507** (2005) 065.

[10] M. Davier, A. Hoecker, B. Malaescu and Z. Zhang, Eur. Phys. J. C **71**, 1515 (2011) [Erratum-ibid. C **72**, 1874 (2012)]; K. Hagiwara, R. Liao, A. D. Martin, D. Nomura and T. Teubner, J. Phys. G **38**, 085003 (2011).

[11] G. W. Bennett *et al.* [Muon (g-2) Collaboration], Phys. Rev. D **73**, 072003 (2006); Phys. Rev. D **80**, 052008 (2009).

[12] T. Moroi, Phys. Rev. D **53**, 6565 (1996) [Erratum-ibid. D **56**, 4424 (1997)]; S. P. Martin and J. D. Wells, Phys. Rev. D **64**, 035003 (2001). G. F. Giudice, P. Paradisi, A. Strumia and A. Strumia, JHEP **1210**, 186 (2012)

[13] I. Gogoladze, F. Nasir, Q. Shafi and C. S. Un, Phys. Rev. D **90**, 035008 (2014).

[14] S. Mohanty, S. Rao and D. P. Roy, JHEP **1309**, 027 (2013); S. Akula and P. Nath, Phys. Rev. D **87**, 115022 (2013); J. Chakrabortty, S. Mohanty and S. Rao, arXiv:1310.3620 [hep-ph].

[15] K. S. Babu, I. Gogoladze, S. Raza and Q. Shafi, Phys. Rev. D **90**, 056001 (2014).

[16] M. Ibe, T. T. Yanagida and N. Yokozaki, JHEP **1308**, 067 (2013).

[17] M. A. Ajaib, I. Gogoladze, Q. Shafi and C. S. Un, JHEP **1405**, 079 (2014).

[18] B. Ananthanarayan, G. Lazarides and Q. Shafi, Phys. Rev. D **44**, 1613 (1991); Phys. Lett. B **300**, 245 (1993); Q. Shafi and B. Ananthanarayan, Proceedings of the Summer School in High Energy Physics and Cosmology 1991, edited by E. Gava, K. Narain, S. Randjbar-Daemi, E. Sezgin, and Q. Shafi, ICTP Series in Theoretical Physics Vol. 8 (World Scientific, River Edge, NJ, 1992).

[19] H. Baer, A. Belyaev, T. Krupovnickas and A. Mustafayev, JHEP **0406**, 044 (2004); K. S. Babu, I. Gogoladze, Q. Shafi and C. S. Un, Phys. Rev. D **90**, 116002 (2014).

[20] M. Carena, I. Low and C. E. M. Wagner, JHEP **1208**, 060 (2012) K. Schmidt-Hoberg, F. Staub and M. W. Winkler, JHEP **1301** (2013) 124; M. Carena, S. Gori, N. R. Shah and C. E. M. Wagner, JHEP **1203** (2012) 014; M. A. Ajaib, I. Gogoladze and Q. Shafi, Phys. Rev. D **86**, 095028 (2012) N. Maru and N. Okada, Phys. Rev. D **87**, no. 9, 095019 (2013); J. Guo, Z. Kang, J. Li and T. Li, arXiv:1308.3075 [hep-ph]. M. Hemeda, S. Khalil and S. Moretti, Phys. Rev. D **89**, no. 1, 011701 (2014). A. Chakraborty, B. Das, J. L. Diaz-Cruz, D. K. Ghosh, S. Moretti and P. Poulose, Phys. Rev. D **90**, no. 5, 055005 (2014); S. Chakraborty, A. Datta and S. Roy, arXiv:1411.1525 [hep-ph].

[21] G. Aad *et al.* [ATLAS Collaboration], "Measurement of Higgs boson production in the diphoton decay channel in *pp* collisions at center-of-mass energies of 7 and 8 TeV with the ATLAS detector," arXiv:1408.7084 [hep-ex].

[22] V. Khachatryan *et al.* [CMS Collaboration], "Observation of the diphoton decay of the Higgs boson and measurement of its properties," arXiv:1407.0558 [hep-ex].

[23] F. E. Paige, S. D. Protopopescu, H. Baer and X. Tata, hep-ph/0312045.

[24] G. Belanger, F. Boudjema, A. Pukhov and A. Semenov, Comput. Phys. Commun. **180**, 747 (2009).

[25] M. Frank, T. Hahn, S. Heinemeyer, W. Hollik, H. Rzehak and G. Weiglein, JHEP **0702**, 047 (2007); G. Degrassi, S. Heinemeyer, W. Hollik, P. Slavich and G. Weiglein, Eur. Phys. J. C **28**, 133 (2003); S. Heinemeyer, W. Hollik and G. Weiglein, Eur. Phys. J. C **9**, 343 (1999); S. Heinemeyer, W. Hollik and G. Weiglein, Comput. Phys. Commun. **124**, 76 (2000).

[26] J. Hisano, H. Murayama , and T. Yanagida, Nucl. Phys. **B402** (1993) 46. Y. Yamada, Z. Phys. **C60** (1993) 83; J. L. Chkareuli and I. G. Gogoladze, Phys. Rev. D **58**, 055011 (1998).

[27] D. M. Pierce, J. A. Bagger, K. T. Matchev, and R.-j. Zhang, Nucl. Phys. **B491** (1997) 3.

[28] J.L. Leva, Math. Softw. 18 (1992) 449; J.L. Leva, Math. Softw. 18 (1992) 454.

[29] J. Beringer *et al.* [Particle Data Group Collaboration], Phys. Rev. D **86**, 010001 (2012).

[30] H. Baer, C. Balazs, and A. Belyaev, JHEP **03** (2002) 042; H. Baer, C. Balazs, J. Ferrandis, and X. Tata Phys. Rev. **D64** (2001) 035004.

[31] T. Aaltonen *et al.* [CDF Collaboration], Phys. Rev. Lett. **100**, 101802 (2008).

[32] E. Barberio *et al.* [Heavy Flavor Averaging Group], arXiv:0808.1297 [hep-ex].

[33] M. A. Ajaib, I. Gogoladze, F. Nasir and Q. Shafi, Phys. Lett. B **713**, 462 (2012).

[34] A. Djouadi, Phys. Rept. **459**, 1 (2008).

[35] J. F. Gunion, H. E. Haber, G. L. Kane and S. Dawson, *"The Higgs Hunter's Guide"*, Addison-Wesley, Reading (USA), 1990.

[36] I. Gogoladze, M. U. Rehman and Q. Shafi, Phys. Rev. D **80**, 105002 (2009).